

Magnetic behavior of electrodeposited cobalt nanowires using different electrolytic bath acidities

V.R. Caffarena^{a,*}, A.P. Guimarães^{b,1}, W.S.D. Folly^{c,2}, E.M. Silva^{d,3}, J.L. Capitaneó^{d,4}

^a *Petróleo Brasileiro S.A. – Petrobras/GE-CORP/TPGE/TPGN, Av. Almirante Barroso, 81–32º andar Centro, Zip Code 20031-004, Rio de Janeiro, Brazil*

^b *Brazilian Physical Research Center (CBPF), CMF, Rua Dr. Xavier Sigaud, 150-Urca, 2290-180 Rio de Janeiro, Brazil*

^c *Universidade Federal de Sergipe, Núcleo de Física, Campus Itabaiana, Itabaiana, SE, Brazil*

^d *Department of Metallurgical and Materials Engineering, COPPE/UF RJ PEMM, P.O. Box 68505, Ilha do Fundão, 21945-970 Rio de Janeiro, RJ, Brazil*

Received 11 December 2006; received in revised form 19 July 2007; accepted 21 July 2007

Abstract

Co nanowires were produced by deposition in porous alumina templates using different electrolytic bath acidities, in order to study the effect on their magnetic properties.

Room temperature FMR measurements and SQUID measurements as a function of temperature showed that the properties of the nanowires are dependent of the bath pH. The results show that the easy magnetization axes change with both temperature and bath acidity.

© 2007 Elsevier B.V. All rights reserved.

Keywords: Magnetic materials; Nanostructures; Electron resonance; Magnetic properties

1. Introduction

Magnetic metallic nanowires are an interesting physical system, with many potential applications, for example in high-density magnetic recording and as sensors [1–4].

It is known that for metals of group 9 and 10 (Co, Ni, and Rh) they always show polycrystalline structures, and the textures are insensitive to the depositing parameters. The polycrystalline growth of metallic nanowires appears to proceed in the typical three-dimensional (3D) nucleation coalescence manner [5,6].

Relative to noble metals, groups 9 and 10 metals have smaller atomic volumes and higher effective electron numbers resulting in a smaller critical dimension for 2D nucleation.

However, Co has much higher melting point and higher binding energy and thus favors the aggregation of atoms into small 3D clusters. The diffusion of electrodeposited atoms along the

surface is inhibited by the high cohesive energy of these metals, resulting in the nucleation, growth, and coalescence of many 3D grains during deposition.

Thus the 3D grains, which form the cobalt nanowire, can have the *c*-axis orientation either parallel or perpendicular relative to the long axis nanowire.

In this study, we have shown systematic changes in the structure of the electrodeposited Co by adjusting these parameters leading to the deposition of Co nanowires with a *c*-axis orientation either parallel or perpendicular to the wires. These changes lead to modifications in magnetic properties due the rotation of the hcp *c*-axis from perpendicular to parallel to the wires.

2. Materials and methods

2.1. Pre-treatment of aluminum foils

The electrochemical cell used in this work for electropolishing and anodizing aluminum, and electrodepositing cobalt, consists of a 600-mL single-compartment glass vessel, an aluminum working electrode and a platinum counter electrode placed in the electrolyte vessel. The distance between the aluminum electrode and platinum electrode was kept at 1 cm.

The current and voltage were monitored throughout the electrochemical process.

Anodic alumina oxide (AAO) films were grown on 99.997% aluminum foil (Vetec) pretreated in a 5% NaOH solution at 60 °C for 60 s, neutralized in 1:1 HNO₃ for 30 s, washed in purified Milli-Q water and etching in HNO₃.

* Corresponding author. Tel.: +55 21 3229 4593; fax: +55 21 3229 4564.

E-mail addresses: valeskac@petrobras.com.br, valeska@cbpf.br (V.R. Caffarena), apguima@cbpf.br (A.P. Guimarães), wfolly@cbpf.br (W.S.D. Folly), elizams@cbpf.br (E.M. Silva), jeff@ima.ufrj.br (J.L. Capitaneó).

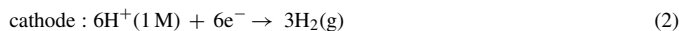
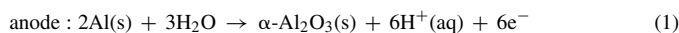
¹ Tel.: +55 21 2141 7183.

² Tel.: +55 21 2290 1615; fax: +55 21 2290 6626.

³ Tel.: +55 21 2290 1615.

⁴ Tel.: +55 21 2562 8265.

The reaction product at the polished Al sheet anode was aluminum oxide, according to the following Eqs. (1) and (2):



2.2. Alumina template

The polished Al sheet was anodized at a constant potential (25 V, in 15 wt% H₂SO₄ at 283 K) and the oxide film formed was dissolved in 1% H₃PO₄ at 333 K for 20 min. The solution could completely dissolve the oxide film, but it did not react with the Al substrate. The partial oxide dissolution in acid is given by Eq. (3):



The Al sheet was then reanodized for 120 h to create the desired long-range ordering. The oxide film was removed in 1% H₃PO₄ for 6 min and the Al sheet anodized again for 30 min.

After anodization, each sample was washed thoroughly with distilled water and dried with an air jet.

2.3. Electrodeposition of cobalt in alumina template and nanowire growth

Cobalt was deposited in the pores of AAO films at two different current densities (50 mA cm⁻² and 5 mA cm⁻²) in an electrolyte consisting of 400 g l⁻¹ of CoSO₄·7H₂O and 40 g l⁻¹ of H₃BO₃ in the electrolyte vessel at 25 °C.

The solution had typical pH values in the range 3.2–3.9, which can be lowered gradually to 2.0 by addition of diluted H₂SO₄, or increased up to 6.0 by addition of NaOH (0.1 M).

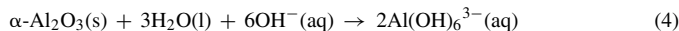
The current and voltage were recorded throughout the electrochemical process using a computer interfaced to an Autolab Potenciostat/Galvanostat Model PGSTAT30 data acquisition/switch unit.

2.4. Characterization

Scanning electron microscopy (SEM) was used to obtain morphological information of the AAO film as well as the size of the pores and interpoles distance.

A portion of a partially dissolved AAO sample (dissolved for only 10 min) was mounted on aluminum supports, coated with a film of gold and submitted to EDX analysis.

Then, the alumite film was completely dissolved in 50 mL of 1.25 M NaOH solution (Eq. (4)), in order to free the cobalt particles from the AAO and obtain a very soluble aluminate, Al(OH)₆³⁻.



After complete dissolution, a drop was put on a silicon substrate and the morphological measurements of the Co nanowire were performed using a Topometrix II[®] atomic force microscope, and Jeol Noran scanning electron microscope.

The crystallographic structure of electrodeposited nanowires was investigated by X-ray diffraction analysis (XRD) using a Miniflex diffractometer with a dwell time of 1° min⁻¹, in the θ –2 θ Bragg–Brentano geometry.

Magnetic hysteresis curves were obtained using SQUID (Quantum Design, Model MPMS) with the external field applied parallel and perpendicular to the nanowires long axis (perpendicular and parallel to the AAO template) in the temperature range 5–300 K. For all the measurements, the SQUID was operated with the superconducting magnet in the dc mode. *M*–*H* and ZFC/FC curves were measured. The nanowires were not removed from the alumina membrane prior to measurement.

FMR spectra were recorded at 9.52 GHz with the magnetic field applied parallel (0°) to the wires in a series of samples using Varian Model E-9. The samples, with 0.5 cm² kept inside the resonance cavity and the measurements were carried out in other directions, to evaluate the magnetic anisotropy of the samples.

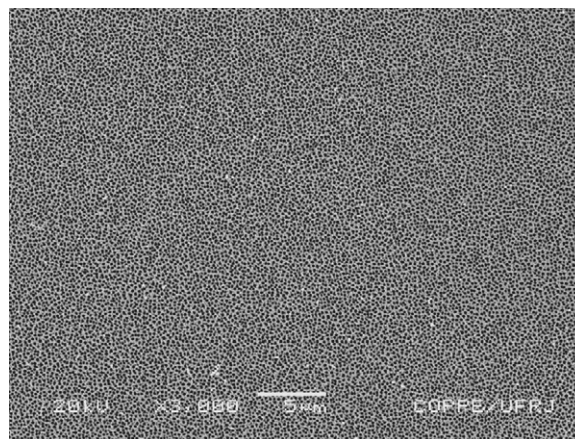


Fig. 1. SEM image of the porous alumina film prepared by two-step anodization with 20 nm diameter pores at 3000×.

3. Results and discussion

3.1. Formation of anodic aluminum oxide films on aluminum

The hexagonally ordered porous alumina templates have been prepared via a two-step anodization process, which was described in detail.

Fig. 1 shows representative SEM images of the pore morphology produced by anodizing aluminum.

As can be seen in Fig. 1, the interpore separation and pore diameter for this sample are about 50 and 20 nm, respectively. A highly ordered aluminum oxide pore structure was obtained in a second anodization step by reanodizing for 30 min.

3.2. Electrodeposition of cobalt into pores of anodic aluminum oxide films

The electrodeposition was carried out at constant current density, in order to that the deposition process could be monitored from the potential response. Cobalt metal is deposited during the cycle as can be confirmed by SEM image in Fig. 2.

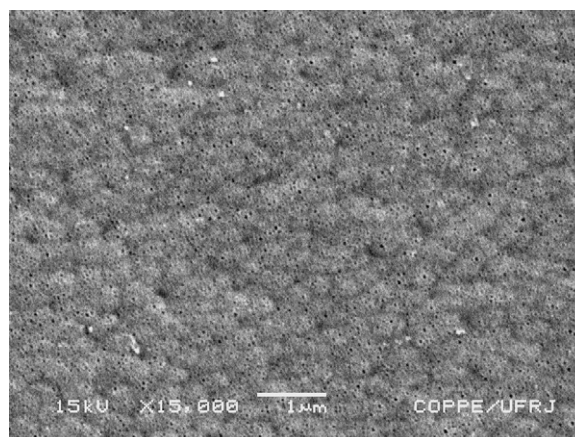


Fig. 2. SEM image of cobalt nanowires into alumina template pores at 15,000×.

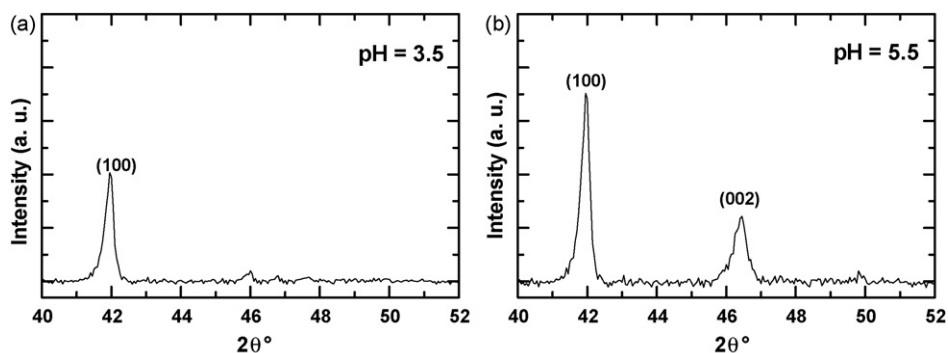


Fig. 3. XRD pattern of Co nanowire arrays obtained in AAM template at pH value of (a) 3.5 and (b) 5.5.

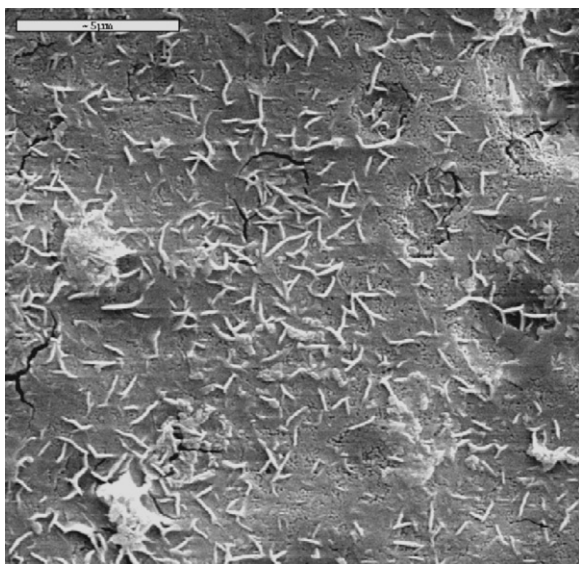


Fig. 4. SEM micrograph of Co nanowires in partially dissolved alumina membrane (1.25 M NaOH/10 min) at 3000 \times .

The XRD pattern for the Co nanowires obtained in the pores of AAO is shown in Fig. 3.

According to the XRD pattern (Fig. 3(a)), for pH 3.5, the existence of (100) peak indicates that the predominant hcp grains have their *c*-axis oriented perpendicular to the axis.

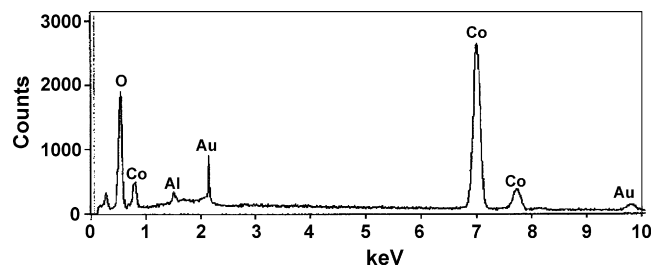


Fig. 6. EDX analysis of cobalt nanowires.

For pH 5.5 (Fig. 3(b)), the (002) peak corresponds to a change in preferred crystallographic *c*-axis to parallel to the wire axis, but the (100) reflection peak are still present.

After dissolving the AAM template in 1.25 mol L⁻¹ NaOH for 10 min, the cobalt nanowire array was put on a silicon substrate and could be seen partly from the template as shown in Fig. 4.

When the dissolving process is complete, after 120 min in NaOH, the visible length of the nanowires becomes longer, 3 μ m, as can be seen in Fig. 5.

The diameter of a nanowire is determined by the pore diameter, and the length is determined from the quantity of the electrodeposited material.

It is seen from the EDX spectrum, Fig. 6, that the nanowires contain only cobalt and oxygen. Al peaks are due to the support,

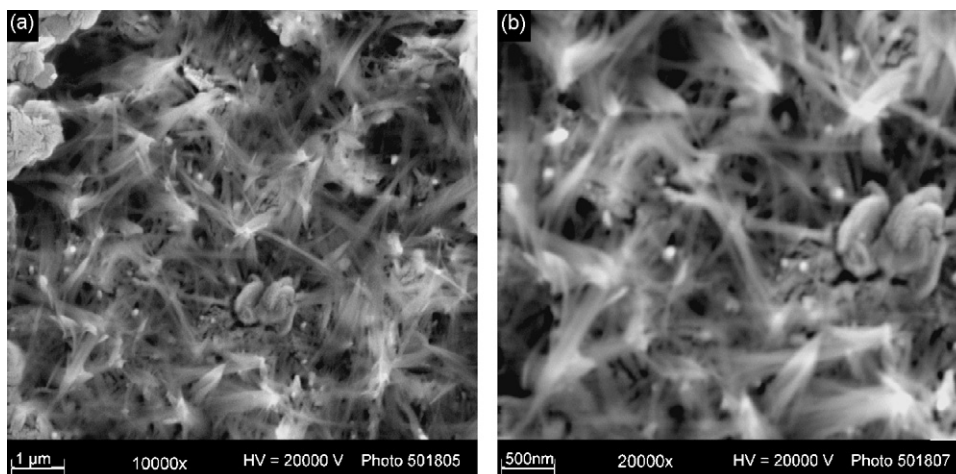


Fig. 5. SEM micrographs of cobalt nanowires, after complete dissolution of alumina membrane.

and the Au peaks to the gold film sputtered on the surface of the sample.

3.3. Magnetic properties of cobalt nanowires (500 A m^{-2} and pH 3.5)

The hysteresis curves were measured parallel and perpendicular to the wire axis at different temperatures. Fig. 7

shows the results for a current density of 500 A m^{-2} and pH 3.5.

Both orientations show only a small hysteretic behavior, resulting in small remanence and coercive field, and suggest that the sample is magnetically hard parallel to the long axis, which is an unusual behavior.

This behavior can be explained considering that the Co deposition proceeds in the 3D nucleation mechanism, which leads to

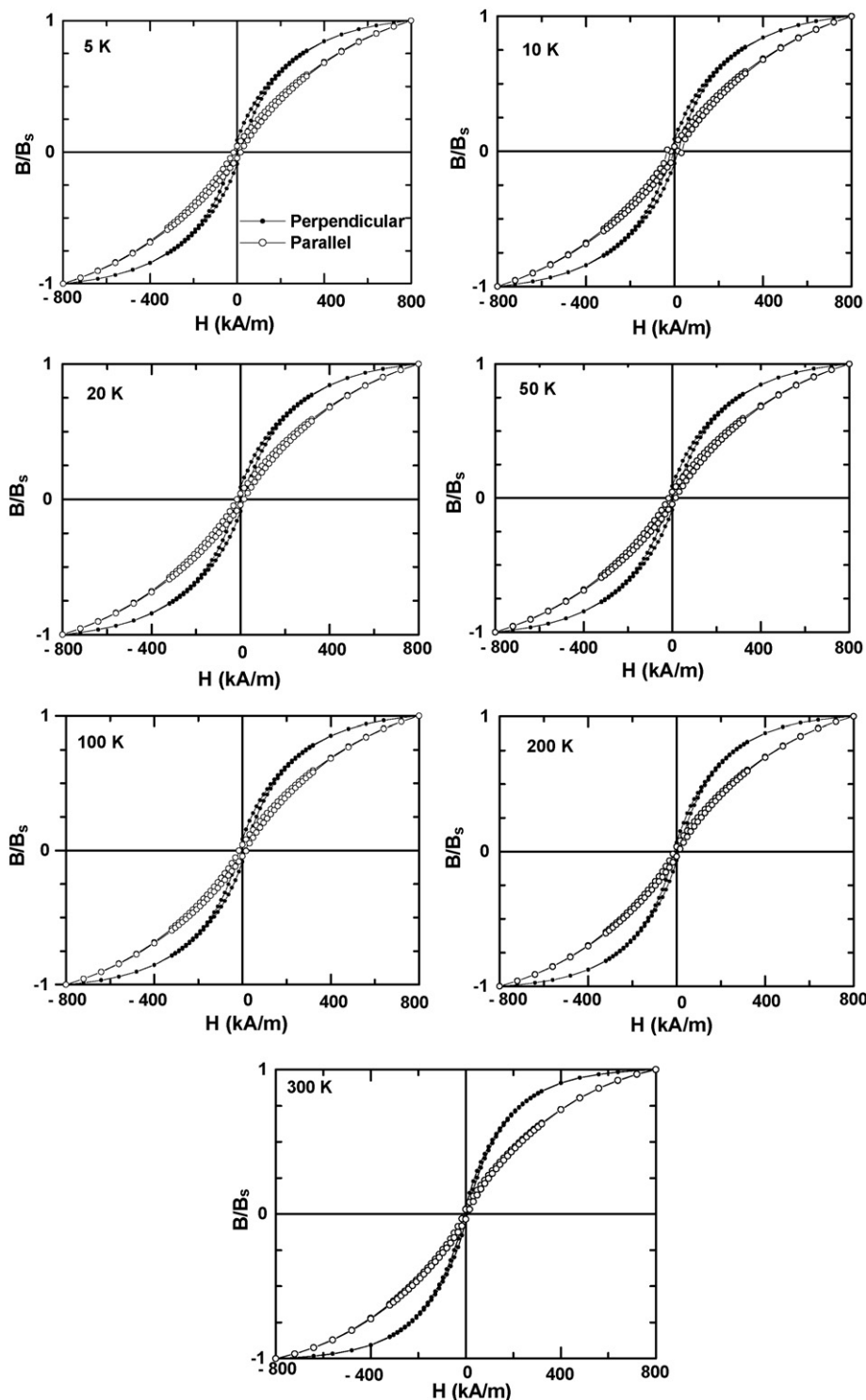


Fig. 7. Hysteresis loops of the array of Co nanowires obtained at pH 3.5, at different temperatures.

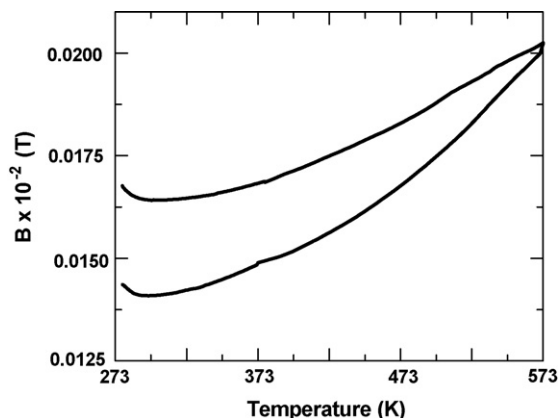


Fig. 8. Zero-field-cooled (ZFC) and field-cooled (FC) magnetization curves at $H = 39.79 \text{ kA m}^{-1}$ for nanowires obtained at pH 3.5.

the coalescence into 3D grains. There are two types of grains in the nanowire: the first type has the axis randomly oriented in a plane perpendicular to the long axis of the wire and, the second type has the axes parallel to the long axis. This result agrees with the XRD pattern showed in Fig. 3, which indicated the existence of two types of grains for the sample.

The SQUID results suggest that the first type of grains is the predominant one for pH 3.5; as consequence, the easy axis is perpendicular to the nanowire long axis.

On the other hand, Fig. 8 shows zero-field-cooled (ZFC) and field-cooled (FC) $M-T$ data for the same sample measured at 39.79 kA m^{-1} . The ZFC and FC curves diverge substantially at low temperatures. This behavior suggests the presence of magnetic nanoparticles in the sample.

The total field acting on each wire is the sum of the applied field and the demagnetizing field of the 2D array. The demagnetizing factor perpendicular to the film plane is 1 for a fully dense infinitely extended film. Taking into account a packing density $P = (d_w/d_c)^2/2\sqrt{3} \times 100$ of 5%, where d_w is the wire diameter and d_c is the center-to-center spacing, the demagnetizing factor is reduced to 0.5 [7–9].

Moreover, in the range 5–20 K, there is a rise in the ZFC/FC curves, which can be attributed to the presence of extremely

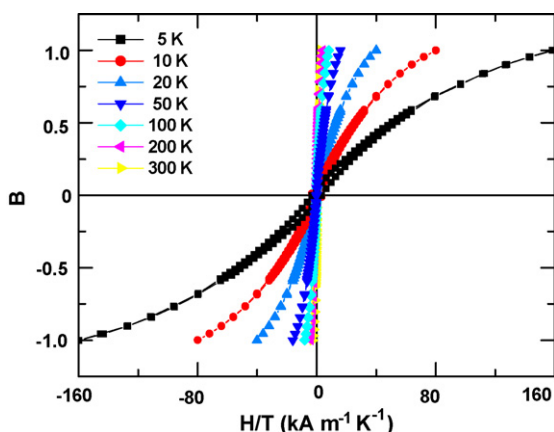


Fig. 9. Magnetization curves at different temperatures plotted as function of H/T .

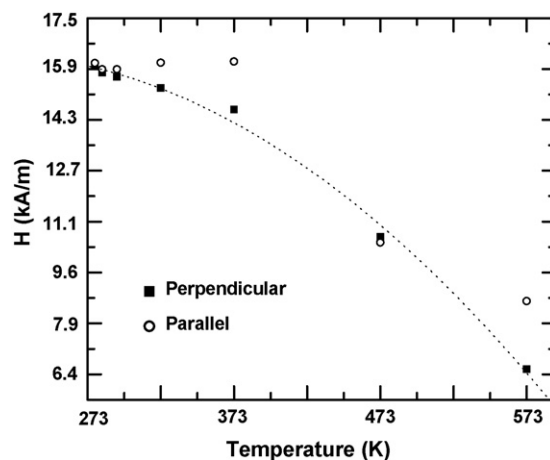


Fig. 10. Coercivity (H_c) of Co nanowires as function of temperature.

small clusters [10,11]. The absence of a clear peak in ZFC curve, with increasing temperature, indicates that the Co clusters in the nanowires have a range of blocking temperatures, as a consequence of range of diameters.

For superparamagnetic samples, the magnetization curves measured above the blocking temperature (T_B) are expected to fall on each other when plotted as a function of H/T . In Fig. 9, the magnetization curves measured at $T > 50 \text{ K}$ clearly merge one another, confirming the occurrence of superparamagnetism above 50 K. From the measured T_B , it is possible to estimate the particle size of the superparamagnetic clusters by using the relation:

$$K_A V = 25 k_B T_B \quad (5)$$

where k_B is the Boltzmann constant. Assuming that the superparamagnetic particles are of metallic cobalt, we estimate the particle diameter, D , to be $\sim 4 \text{ nm}$, corresponding to $T_B = 50 \text{ K}$.

In Fig. 10, we observe that the coercive fields (H_c) become larger as the temperature (T) decreases with folds both parallel and perpendicular to the long axis.

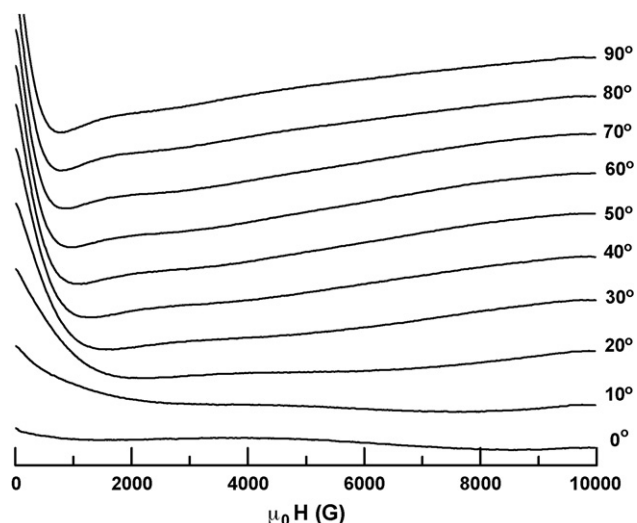


Fig. 11. FMR measurements of Co nanowires performed at room temperature.

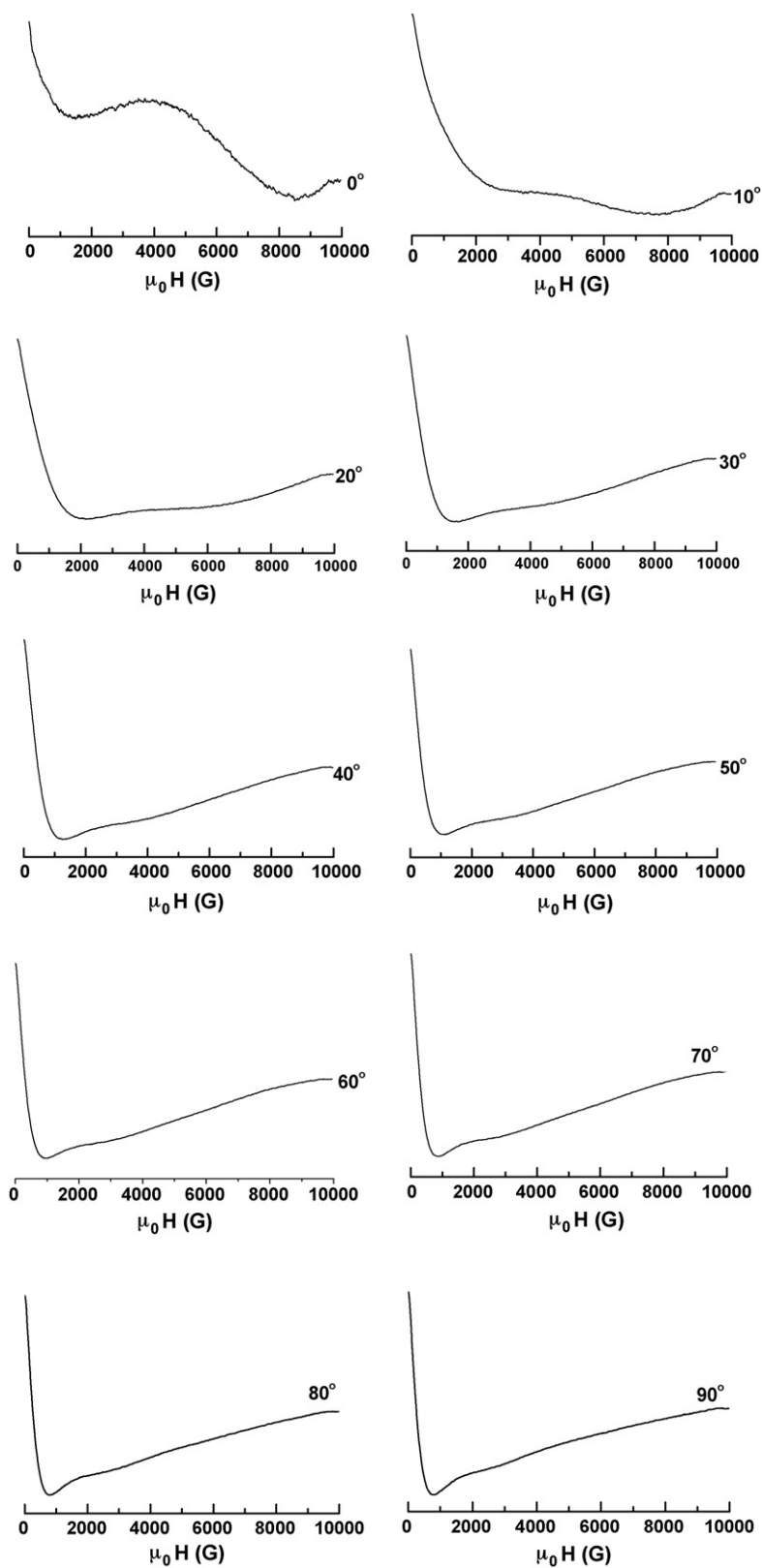


Fig. 12. Angular-dependent FMR lines of Co nanowires.

This behavior confirms that the effects of the temperature only shift the whole graphs and, consequently, the higher temperature usually give smaller coercivity [12] as can be observed in Fig. 10.

Ferromagnetic resonance has been used in order to obtain complementary information on the magnetic properties of these nanowires. Fig. 11 presents the absorption derivative, measured

at a frequency of 9.52 GHz, while sweeping the magnetic field parallel to the wires.

FMR studies supplies information about fundamental magnetic magnitudes as spontaneous magnetization, gyromagnetic factor, but also on magnetic anisotropy, another factor of interest in this study.

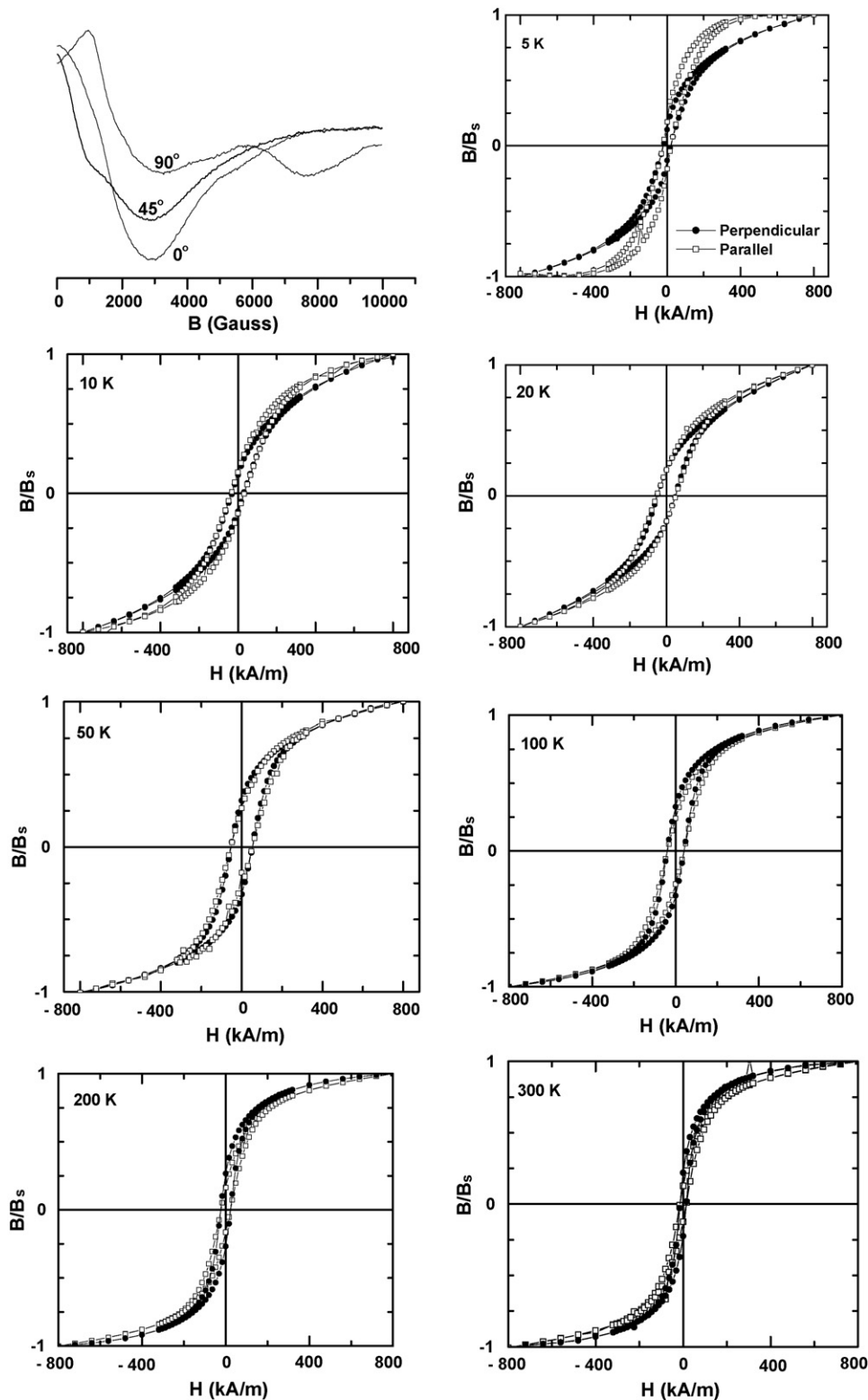


Fig. 13. FMR measurements and hysteresis loops of the array of Co nanowires obtained at pH 5.5.

As can be seen from Fig. 11, the results of the FMR measurements agree with those from the SQUID measurements, indicating that the easy axis is perpendicular to the wire axis.

The FMR spectra show in detail (Fig. 12), exhibit considerable anisotropic behavior as the field is rotated both in the sample plane and from the film plane towards the film normal direction.

As can be seen from figure, the hard axis of the surface anisotropy is parallel to the nanowire axis. The lowest resonance field is measured at 90° , while the maximum resonance field is observed at 0° (parallel to the nanowires). This behavior is consistent with Co grains having their *c*-axis perpendicular to the wires.

3.4. Magnetic properties of cobalt nanowires (500 A m^{-2} and pH 5.5)

The pH was increased gradually up to 5.5 by addition of NaOH 0.1 M and the electrodeposition was carried out using this solution and the same current density employed in the first condition (500 A m^{-2}).

The FMR and SQUID measurements (Fig. 13) suggest that as the pH is varied, the preferential structural phase, hcp grains with their *c*-axis oriented perpendicular to the wires, changes to a disordered structural phase.

These results indicate the increase in the fraction of grains having their *c*-axis parallel to the wires. However, for this value pH of the fraction of Co grains with *c*-axis perpendicular still dominates and, consequently, the easy axis is perpendicular to the long axis.

When the temperature decrease the parallel axis becomes the easy one, as can be seen in Fig. 13. At temperatures below 50 K, the hard axis is the perpendicular axis and this behavior is different in relation to the sample obtained at pH 3.5.

May thus concluded that the fraction of Co grains with the *c*-axis parallel to the wire axis increases for pH 5.5 and there are superparamagnetic grains blocked above 50 K.

The FMR absorption peaks at 90° and 0° indicate that the magnetic anisotropy decreases with pH increase. A substantial increase in the coercive field (H_c) is observed at high pH solution, which favors a *c*-axis parallel to the wires.

4. Conclusions

We have prepared cobalt nanowires with diameter of about 20 nm and length of 3 μm , using the electrodeposition method and developed a systematic study of the influence of temperature and electrolytic acidity on this magnetic properties.

The XRD, SEM and EDX analysis were used to characterize them. Morphologic observations indicate that the nanowires are uniform in size and shape, which confirms that electrodeposition is a good procedure to make these 1D nanostructures.

FMR and SQUID measurements show that, depending on the choice of pH and current density, different magnetic properties can be obtained. The control of these properties in cobalt nanowires should be useful in their potential applications in perpendicular recording media.

The magnetization curves and the FMR properties show that the anisotropy properties of Co nanowires depend on the pH of the solution due to the induced changes in the microstructure. At pH 3.5, a considerable fraction of grains are grown with their *c*-axis aligned perpendicular to the wire axis, whereas an increase of pH (5.5) seems to favor the deposition of *c*-axis aligned parallel to the wires. Then, very different magnetic properties can be obtained simply changing the electrolytic bath acidity.

Acknowledgements

The authors thank FAPERJ for the financial support and Petr leo Brasileiro S.A., CBPF, CEPEL and PEMM-COPPE/UFRJ for the use of the experimental facilities.

References

- [1] T.M. Whitney, J.S. Jiang, P.C. Searson, C.L. Chien, *Science* 261 (1993) 1316–1319.
- [2] R.S. Friedman, M.C. McAlpine, D.S. Ricketts, D. Ham, C.M. Lieber, *Nature* 434 (2005) 1085.
- [3] M. Yun, N.V. Myung, R.P. Vasquez, J. Wang, H. Monbouquet, in: E.A. Dobisz (Ed.), *SPIE Proceedings* 5220, 2003.
- [4] G. Zheng, F. Patolsky, Y. Cui, W. Wang, C.M. Lieber, *Nat. Biotechnol.* 23 (2005) 1294–1301.
- [5] M. Tian, J. Wang, J. Kurtz, T.E. Mallouk, M.H.W. Chan, *Nano Lett.* 3 (2003) 919–923.
- [6] M. Darques, A. Encinas, L. Vila, L. Piraux, *J. Phys. D: Appl. Phys.* 37 (2004) 1411–1416.
- [7] T.A. Crowley, K.J. Ziegler, D.M. Lyons, D. Erts, H. Olin, M.A. Morris, J.D. Holmes, *Chem. Mater.* 15 (2003) 3518–3522.
- [8] H. Forster, T. Schrefl, R. Dittrich, D. Suess, W. Scholz, V. Tsiantos, J. Fidler, K. Nielsch, H. Hofmeister, H. Kronm ller, S. Fischer, *IEEE Trans. Magn.* 38 (2002) 2580–2582.
- [9] D.J. Sellmyer, M. Zheng, R. Skomski, *J. Phys.: Condens. Mater.* 13 (2001) R433–R460.
- [10] G.A. Jones, C.A. Faunce, D. Ravinder, H.J. Blythe, V.M. Fedosyuk, *J. Magn. Mater.* 184 (1998) 28–40.
- [11] H.J. Blythe, V.M. Fedosyuk, O.I. Kasyutich, W. Schwarzacher, *J. Magn. Mater.* 208 (2000) 251–254.
- [12] C. Chang, J. Yang, *J. Magn. Mater.* 155 (1996) 92–94.